Hydroxyl Terminated Poly(ether ether ketone) with Pendant Methyl Group-Toughened Epoxy Clay Ternary Nanocomposites: Preparation, Morphology, and Thermomechanical Properties

A. Asif, K. Leena, V. Lakshmana Rao, K. N. Ninan

Thermoplastic Polymers Section, Polymers and Special Chemicals Division, Propellants and Special Chemicals Group, Propellants Chemicals and Materials Entity, Vikram Sarabhai Space Centre, Trivandrum-695 022, India

Received 31 August 2006; accepted 27 February 2007
DOI 10.1002/app.26774
Published online 9 August 2007 in Wiley InterScience (www.interscience.wiley.com).

ABSTRACT: Hydroxyl terminated poly(ether ether ketone) oligomer with pendant methyl group (PEEKMOH) was prepared. Ternary nanocomposites were processed by blending PEEKMOH oligomer with diglycidyl ether of bisphenol-A (DGEBA) epoxy resin along with organically modified montmorillonite (Cloisite 25A) followed by curing with 4,4′-diamino diphenyl sulfone. Tensile moduli and flexural moduli were increased, while the tensile strength and Izod impact strength were decreased with increase in clay content. Similarly, storage moduli and loss moduli were increased and glass transition temperature was decreased as the percentage of clay increased. X-ray diffractograms showed exfoliated morphology even with higher concentration of clay content (8 phr). Scanning electron microscopy of fractured surfaces and tensile failed specimens revealed slow crack propagation and increase in river markings with nanoclay incorporation confirming the improvement in toughness. The domain size of PEEKMOH was decreased with the incorporation of nanoclay into the epoxy matrix, indicating the restriction of growth mechanism by nucleation during phase separation. With increase in clay content, phase separation disappeared indicating gelation occurs before phase separation. Fracture toughness was increased with the addition of PEEKMOH and clay in epoxy resin. Coefficient of thermal expansion of nanocomposites decreases up to 3 phr clay concentrations thereafter it increases. A marginal increase in thermal stability was observed with increase in clay content. © 2007 Wiley Periodicals, Inc. J Appl Polym Sci 106: 2936–2946, 2007

Key words: epoxy resin; PEEKMOH; ternary nanocomposite

INTRODUCTION

Polymer-layered silicate nanocomposites have attracted great interest, both in industry and in academics, because they often exhibit remarkable improvement in material properties compared with virgin polymer or conventional micro and macrocomposites.[1–6] Conventional composites usually require a high content (>10%) of the inorganic fillers to impart the desired mechanical properties. Such high filler levels increase their density of the product and can cause the deterioration in properties through interfacial incompatibility between the filler and the organic material. Besides, processability worsens as filler content increases. In contrast, nanocomposites show enhanced thermomechanical properties even with a small amount of layered silicate (≤5%).[7] Improvements comprise higher modulus, increased strength, heat resistance, decreased gas permeability, reduced coefficient of thermal expansion, and decreased flammability.[1–6,8] The main reason for this improved property in nanocomposites is the ultra large interfacial interaction between the matrix and layered silicate and also the high aspect ratio of the dispersed clay particles. NASA reported that polymer clay nanocomposites are the potential candidates for cryogenic storage bottles due its high barrier property.[9]

Among polymer-layered silicate nanocomposite, epoxy-based systems have been studied extensively by several researchers.[10–20] There are many factors, which influence the morphology of nanocomposites, for instance nature of curing agent, nature of clay, curing conditions, processing method, etc. It was found that when anhydride was used as curing agent, there was an exfoliated morphology, while diamino diphenyl methane (DDM) gave an intercalated morphology, since anhydride is a liquid, which can easily diffuse to the gallery, whereas DDM was a solid.[10] Similar observations were observed by Xu et al.[11] for diethylenetriamine and Tung oil anhydride. Kornman et al.[12] found that aliphatic amine-cured epoxy produced an exfoliated morphology compared to cyclo aliphatic amine because of the lower reactivity of later. The diffusion rate and reactivity of the curing agent also influence the exfoliation of clay.

Correspondence to: V. L. Rao (v_lakshmanarao@vssc.gov.in).

Journal of Applied Polymer Science, Vol. 106, 2936–2946 (2007)

Intercalated nanocomposite is generally produced with quaternary and tertiary alkyl ammonium surfactants that do not contain hydroxyl groups, because of the low Bronsted acidity of the surfactants.[5,13] The fixed layer separation of clay layers is unable to provide optimum level of reinforcement. Exfoliated nanocomposite is produced with primary and secondary alkyl ammonium surfactants or quaternary surfactants containing hydroxyl groups, because of the high Bronsted acidity of the surfactants.[5,13] The clay layers will be sufficiently separated and randomly oriented to allow full interfacial bonding and to contribute all of their strength to improve the properties of nanocomposites. The Bronsted acidity of clay modifier catalyzes epoxy amine polymerization. Lan et al.[13] reported that as the chain length of alkyl ammonium (clay modifier) increases, the morphology changes from intercalation to exfoliation morphology.

The processing conditions also affect the clay morphology. The usual processing methods to disperse the clay layers in epoxy matrix are mechanical stirring, ultrasound sonication,[14–16] high shear mixing,[16–18] ball milling,[19] etc. Lam et al.[15] found that 10-min ultrasonication was found to give an optimum microhardness at 4 wt % clay containing epoxy nanocomposites. For PMMA/Clay and PP/PS-Clay nanocomposites, it was realized that ultrasonic-assisted melt-mixing successfully generated exfoliated nanocomposites compared to *in situ* polymerization, which greatly affected the performance of nanocomposites.[14] Zunjarrao et al.[16] reported that high speed shear mixing resulted in better dispersion of clay particles and better mechanical properties rather than ultrasonication, even if both methods gave exfoliated morphology. It was reported that 4,4′-diamino diphenyl sulfone (DDS)-cured epoxy nanocomposites showed an exfoliated morphology with improved mechanical properties when dispersed through exerting shearing force on epoxy montmorillonite solution by ball milling.[19] The toughening effects of thermoplastic[21–24] and nanoclay[25] separately on the thermomechanical properties of epoxy systems have been studied enormously. However, no evidence of drastic increase in fracture toughness was reported in the open literature for epoxy clay nanocomposites. On the other hand, more than 100% increase in fracture toughness was observed by us[23,24] and others[26–32] for the thermoplastic-toughened epoxy systems. Frohlich et al.[33] reported the improved toughness in rubber-toughened hybrid epoxy nanocomposites compared with nanocomposite without rubber. The T_g was lowered drastically due to the presence of rubber. Balakrishnan et al.[34] observed that the ductility of epoxy resin was enhanced without considerable reduction in the modulus and strength when organoclay and rubber dispersants were added to epoxy resin. Isik et al.[35] studied the mechanical properties of epoxy-polyetherpolyol-organically treated montmorillonite nanocomposite with respect to polyetherpolyol content and clay content. They observed an increased T_g and Young's modulus with respect to clay content. Peng et al.[36] investigated the impact of clay on the phase morphology of epoxy/poly(ether imide) ternary hybrid nanocomposites, but the reports based on the hybrid effect of both functionalized thermoplastic and nanoclay together on epoxy systems have not been reported in detail. Hence, we report here the hydroxyl-terminated poly(ether ether ketone) with pendant methyl group-toughened epoxy clay ternary nanocomposites and its morphology and thermomechanical properties.

EXPERIMENTAL

Materials

High purity methyl hydroquinone (MeHQ) (Aldrich); 4,4′-difluoro benzophenone (DFBP) (Spectrochem, India); anhydrous potassium carbonate (BDH, India); *N*-methyl-2-pyrrolidone (NMP) (SRL, India), Toluene (Qualigens, India) were used for the synthesis of modified PEEK. MeHQ and DFBP were vacuum-dried at 70 and 60°C, respectively. Anhydrous potassium carbonate was dried at 400°C in a muffle furnace before use. NMP was distilled under reduced pressure over P_2O_5 and stored over molecular sieves. Toluene was distilled over sodium and stored over sodium wire DGEBA epoxy resin (LY 556, Ciba Geigy) with an epoxide equivalent weight of 188.68 was used. High purity 4,4′-diamino diphenyl sulphone (DDS) (Merck) was used as received. Tri phenyl phosphine (TPP) (Aldrich) was dried and used. Cloisite 25A (Southern Clay Product) [dimethyl hydrogenated tallow (2-ethyl hexyl) quaternary ammonium modified montmorillonite, d_{001} = 18.6 Å, CEC = 95 mequiv/100 g clay, specific gravity =1.87 g/cc] was dried under vacuum at 70°C before use.

Synthesis of PEEKMOH oligomer

Hydroxyl terminated PEEK oligomer having pendant methyl groups with number–average molecular weight ($\bar{M}_n$) = 12,000 (Theoretical) was synthesized by aromatic nucleophilic displacement of fluorine from an activated substrate, 4,4′-difluoro benzophenone (DFBP) by methyl hydroquinone (MeHQ) as per Scheme 1. The molecular weight was controlled by taking specified amount of monomers calculated using Carother's equation as given in Eq. (1).[37,38] The hydroxyl functional group was maintained by taking calculated excess of the dihydroxy monomer, MeHQ. The procedure for the synthesis of hydroxyl terminated PEEKMOH oligomer with number average molecular weight ($\bar{M}_n$) 12,000 is as follows. The synthesis was conducted in a clean and dry four-necked flask equipped with a mechanical stirrer, thermowell,

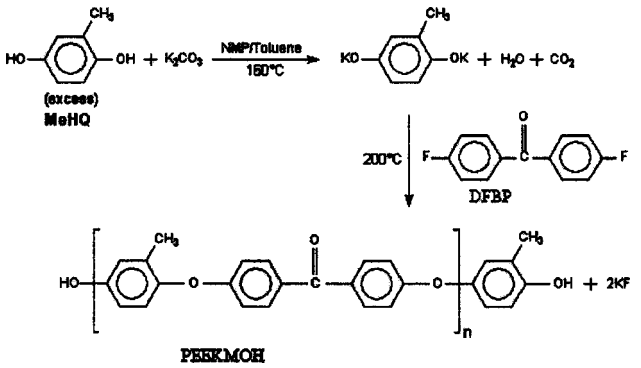

Scheme 1 Reaction scheme for the synthesis of hydroxyl-terminated PEEK with pendent methyl group.

nitrogen inlet, and Dean-Stark trap outfitted with a condenser. The flask was purged with dry nitrogen before starting the reaction. The flask was charged with 35 g (0.2819 mols) of MeHQ and 44.46 g (0.3217 mols) of potassium carbonate. Potassium carbonate was used as a catalyst. The compounds were carefully washed into the flask using 367.5 mL of NMP. Hundred and fifty milliliters of toluene was added to the solution as azeotroping agent. The reaction mixture was heated at 160°C for 4 h with constant stirring. Water formed during reaction was removed as an azeotrope with toluene through the Dean-Stark trap. After 4 h, the reaction temperature was brought down to 100°C and 58.4994 g (0.2681 mols) of DFBP and 100 mL NMP were added to the flask. The reaction mixture was heated at 200°C with constant stirring for 3 h and cooled to room temperature. The polymer formed was precipitated by adding distilled water at room temperature. Complete precipitation was ensured by heating the solution at 60°C with constant stirring. The precipitated oligomer was filtered, purified by reflection with water, followed by sauxhlet extraction with acetone and dried under vacuum at 120°C for 24 h.

$$\langle \bar{X}_n \rangle = \frac{1+r}{1-r} \quad (1)$$

where $\langle \bar{X}_n \rangle$ = number average degree of polymerization; $r = N_A/N_B < 1$, where N_A and N_B are the number of moles of monomers having bifunctional groups of type A (i.e., flourine) and type B (i.e., hydroxyl), respectively.

Preparation of PEEKMOH-toughened epoxy clay ternary nanocomposites

PEEKMOH-toughened epoxy clay ternary nanocomposites were prepared as per the Scheme 2.

Characterization

The ^{13}C NMR spectrum of the PEEKMOH oligomer was recorded using Bruker Avance-300 spectrometer using deuteriated chloroform ($CDCl_3$) as a solvent and tetramethyl silane as an internal standard.

FTIR analysis

Infrared studies were conducted to investigate the completion of curing reaction. Fully cured samples were powdered and the spectra of these samples in KBr pellets were recorded using a Perkin–Elmer Spectrum GXA FTIR spectrometer.

Wide angle X-ray spectroscopy

Wide angle X-ray scattering (WAXS) data were obtained on powder samples of the polymer using a PANalytical model X-ray diffractometer with Xpert pro software and nickel-filtered Cu-Kα radiation at 30 kV and 20 mA. Samples were recorded at room temperature over the 2θ angular range of 2–30°.

Fracture toughness, tensile and flexural properties

Fracture toughness, Tensile and flexural properties were determined as per ASTM 5045, ASTM D638, and ASTM D790, respectively. The measurements were done using a universal testing machine (Model TNE 5000) at a crosshead speed of 10 mm/min. Rectangular specimens of 100 × 10 × 3 mm^3 were used for determining flexural strength. Flexural modulus was determined from the slope of the initial portion of the flexural stress–strain curve.

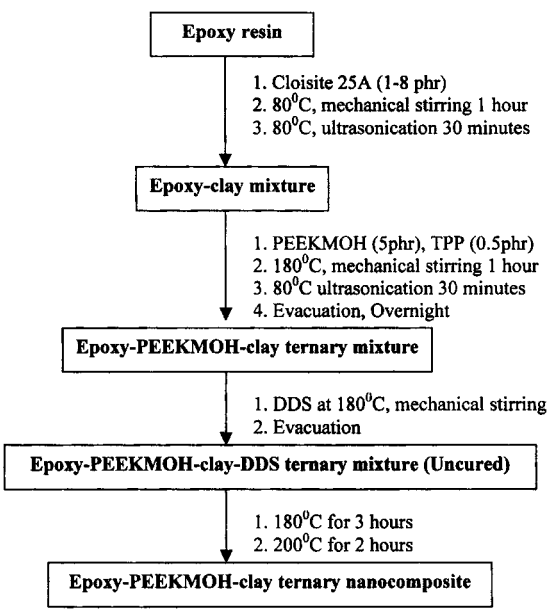

Scheme 2 Process chart for the preparation of PEEKMOH-toughened epoxy clay ternary nanocomposite.

Flexural strength was calculated using the equation

$$\text{Flexural strength} = \frac{3PL}{2bd^2} \quad (2)$$

where P is the load at break and L is the span length; b and d are the breadth and thickness of the specimen, respectively. Dog bone-shaped specimens were used for tensile properties evaluation.

Single edge notch specimens of 46 × 6 × 3 mm^3 (span length =24 mm) were used to measure the fracture toughness of epoxy clay ternary nanocompsoites. A notch of 2.7 mm was made at one edge of the specimen. A natural crack was made by pressing a fresh razor blade into the notch. The fracture toughness was expressed as stress intensity factor (K_{IC}) calculated using equation

$$K_{IC} = \frac{P}{BW^{1/2}} f(x) \text{ where } (0 < x < 1) \quad (3)$$

$$f(x) = 6x^{1/2} \frac{[1.99 - (1-x)(2.15 - 3.93x + 2.7x^2)}{(1+2x)(1-x)^{3/2}}$$

P is the load at the initiation of crack; B is the specimen thickness; W is the specimen width; a is the crack length and $x = a/w$.

Izod impact energy and strength

The Izod impact energy and strength were determined using Tinius Olsen model impact 503 machine with weight set pendulum as per ISO 180. Rectangular specimens of 80 × 10 × 4 mm^3 were used for determining Izod impact energy and strength with a notch depth of 2 mm.

Scanning electron microscopy

The morphology of the cryogenically fractured/tensile-failed surfaces were analyzed using Philips XL 20 scanning electron microscope. The failed surfaces were etched with chloroform for 24 h to remove the thermoplastic phase. The specimens were dried in vacuum overnight to remove the solvent. All the specimens were sputter-coated with gold before taking the micrographs.

Dynamic mechanical thermal analysis

The viscoelastic properties of the unmodified resin as well as the nanocomposites were measured using TA Instruments DMA 2980 dynamic mechanical thermal analyzer. Rectangular specimens of 50 × 10 × 3 mm^3 were used for the analysis. The analysis was done in three-point bending mode at a frequency of 1 Hz from room temperature to 300°C at a heating rate of 2°C/min.

Thermomechanical analysis

Thermomechanical analyzer (Perkin Elmer TMA-7) is used to determine the coefficient of thermal expansion (CTE) and the glass transition temperature (T_g). It consists of a highly sensitive linear variable differential transformer, low mass furnace, and a precise motor for probe loading. Samples were run at a heating rate of 10°C/min from room temperature to 250°C under N_2 atmosphere.

Thermogravimetric analysis

The thermal stability of the nanocomposites was analyzed by thermogravimetric analysis using TA Instruments model SDT 2960 thermal analyzer. The samples were heated from room temperature to 900°C at a heating rate of 10°C/min in nitrogen atmosphere.

RESULTS AND DISCUSSION

The FTIR spectrum of PEEKMOH (Fig. 1) shows characteristic absorption at 1220–1225 cm^{-1} due to symmetrical stretching vibration of ϕ–O (phenyl-ether) bond and 1600–1650 cm^{-1} due to stretching vibration of carbonyl group. The aromatic C–H stretching was observed at 3038 cm^{-1}. Absorption at 2960 cm^{-1} was due to the C–H stretching vibration of the methyl groups. The presence of a broad band between 3000 and 3500 cm^{-1} confirmed the presence of hydroxyl groups.[23] The C^{13} NMR spectrum of PEEKMOH along with the peak assignments is shown in Figure 2. The spectrum revealed twelve peaks corresponding to twelve distinguishable carbon atoms in the oligomer. The chemical shift assignments of various carbon atoms were based on the additivity constants for substituted benzene. The peak due to carbonyl carbon is seen in the 190–200 ppm range. The methyl carbon peak was observed in 10–20 ppm range. The other

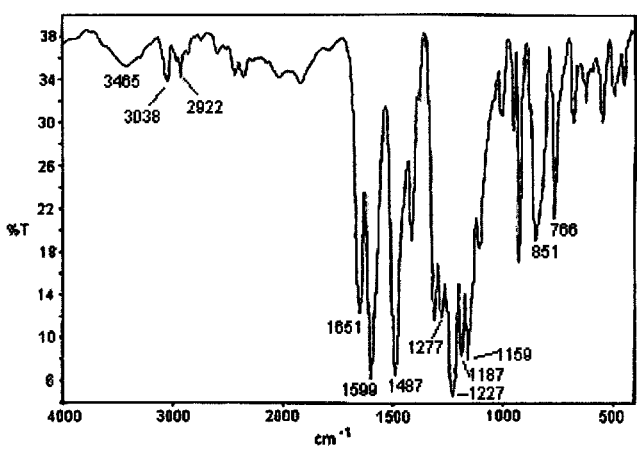

Figure 1 FTIR spectrum of PEEKMOH.

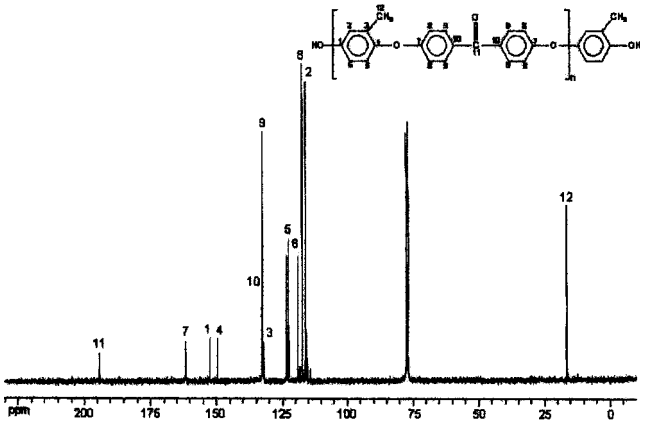

Figure 2 ^{13}C NMR spectrum of PEEKMOH.

peaks in the spectrum were due to aromatic ring carbons of the polymer.

FTIR studies

The IR spectrum of the nanocomposite is given in Figure 3. The epoxy peak at 914 cm^{-1} vanished after the curing indicating that the cure reaction reaches completion.

Wide angle X-ray diffraction

To corroborate the nature of the clay inside the ternary nanocomposites, the diffraction pattern of the pristine Cloisite 25A was compared with the diffraction pattern of the nanocomposites having different clay fractions in Figure 4. The virgin clay Cloisite 25A has the *d*-spacing value of 18.1 A° at $2\theta = 4.87°$. No prominent peak was observed in the diffraction pattern of any of the ternary nanocomposites even for higher phr of Cloisite 25A. This indicated the complete exfoliation of clay in all the nanocomposites. Park and Jana[39] also observed an exfoliated morphology for aromatic epoxy DDS nanocomposite containing 4 wt % of quaternary ammonium modified clay. Zunjarrao et al.[16] also observed similar exfoliation by ultrasonication. In the present study, mechanical stirring and ultrasonication along with high temperature mixing and curing helped for the complete exfoliation of clay.

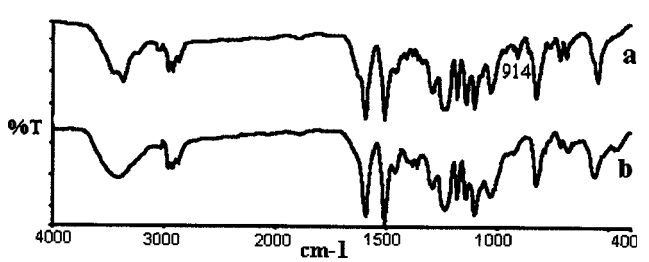

Figure 3 IR spectrum of PEEKMOH (5 phr)-toughened epoxy clay (5 phr) ternary nanocomposite: (a) before curing and (b) after curing.

Fracture toughness, tensile and flexural properties

Fracture toughness, tensile and flexural properties of the PEEKMOH toughened epoxy and PEEKMOH toughened epoxy clay ternary nanocomposites are given in Table I. Data reveals that there is a marginal decrease in both tensile modulus and flexural modulus with the addition of PEEKMOH oligomer to the epoxy/DDS system. Similar observation was made by us earlier for epoxy–hydroxyl terminated tertiary butyl PEEK[24] and epoxy–hydroxyl terminated methyl PEEK systems.[23] It is known that the incorporation of clay into the epoxy matrix enhances tensile modulus and flexural modulus to a great extent. Basara et al. observed 17.2% increase in tensile modulus when 7 wt % of Cloisite 30B was incorporated to epoxy matrix.[40] In the present system, it was observed that moduli increases with increases in clay content even with the presence of PEEKMOH oligomer. The increase was observed to the tune of 20 and 10% in tensile modulus and flexural modulus, respectively with the incorporation of 8 phr clay content to 5 phr PEEKMOH toughened epoxy matrix with respect to epoxy matrix, whereas the increase in tensile moduli and flexural moduli were found to be 27 and 14%, respectively with respect to PEEKMOH-toughened epoxy matrix. This may be explained in terms of strong interactions between polymer matrix and rigid silicate layers and also due to the nanodispersion of rigid silicate layers in the epoxy matrix. Isik et al.[35] also found similar increment in tensile modulus for polyether polyol-modified epoxy montmorillonite ternary nanocomposite. However, there is a marginal decrease in tensile strength as the clay content increases. There are several reasons to explain the decrease in tensile strength as clay content increases.

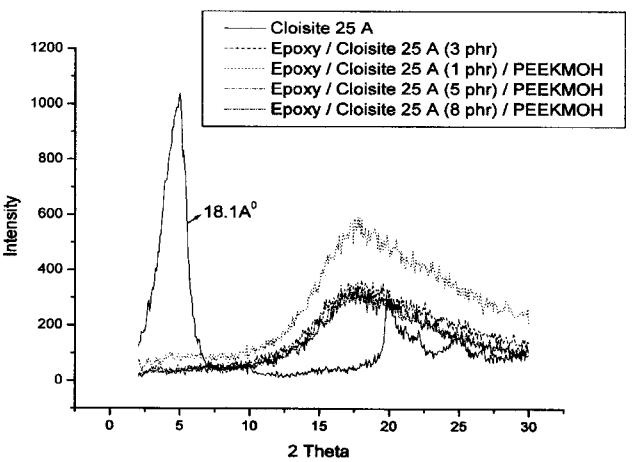

Figure 4 X-ray diffraction pattern of nanocomposites.

TABLE I
Fracture Toughness, Tensile and Flexural Properties of Epoxy Clay Ternary Nanocomposites

Composition	Tensile modulus (GPa)	Tensile strength (MPa)	Flexural modulus (GPa)	Flexural strength (MPa)	Fracture toughness (MPa $m^{1/2}$)	% Strain at break
Neat epoxy	1.53 ± 0.02	63 ± 4	2.95 ± 0.11	122 ± 6	1.16 ± 0.16	3.4 ± 0.3
Epoxy/PEEKMOH	1.44 ± 0.04	72 ± 6	2.86 ± 0.12	112 ± 6	2.17 ± 0.19	9.3 ± 0.2
Epoxy/Cloisite 25A (3 phr)	1.57 ± 0.01	64 ± 7	3.08 ± 0.09	97 ± 11	1.29 ± 0.20	4.1 ± 0.4
Epoxy/Cloisite 25A (1phr)/PEEKMOH	1.54 ± 0.01	65 ± 2	3.06 ± 0.02	110 ± 2	1.59 ± 0.11	6.8 ± 0.2
Epoxy/Cloisite 25A (3phr)/PEEKMOH	1.60 ± 0.01	59 ± 1	3.09 ± 0.05	105 ± 10	1.42 ± 0.10	5.4 ± 0.1
Epoxy/Cloisite 25A (5phr)/PEEKMOH	1.67 ± 0.04	55 ± 1	3.24 ± 0.02	109 ± 7	1.39 ± 0.11	5.0 ± 0.3
Epoxy/Cloisite 25A (8phr)/PEEKMOH	1.83 ± 0.02	48 ± 4	3.25 ± 0.03	108 ± 5	1.32 ± 0.10	4.7 ± 0.1

One reason is the stress concentration effect of agglomerated clay particles at higher clay loadings. The agglomeration of clay particles at high clay concentration also results lower in tensile strength due to lowering of filler surface area and lower polymer/clay surface interaction. Another reason is that as clay content increases, the viscosity of the system increases resulting in heterogeneity and nanovoids formation due to the entrapment of air bubbles during sample preparation. Similar observations are noticed in polyether polyol-modified epoxy montmorillonite ternary nanocomposite[35] and other epoxy montmorillonite nanocomposites.[40,45] No noticeable change was observed in flexural strength as clay content increases.

From the Table I, it reveals that percentage strain at break and fracture toughness values were found to be higher for PEEKMOH-toughened epoxy clay ternary nanocomposites compared to neat epoxy resin. However, as the clay content increases, percentage strain at break and fracture toughness decreases for ternary nanocomposites revealing that the thermoplastic is the main contributing factor for the increase in percentage strain at break and toughness of the nanocomposites rather than the clay alone. The increase in fracture toughness and percentage strain at break is found to be marginal for epoxy clay nanocomposites without the addition of thermoplastic. The percentage strain at break and fracture toughness was found to be maximum for PEEKMOH-toughened epoxy system without clay.

Izod impact energy and strength

The Izod impact energy and strength of the epoxy clay ternary nanocomposites are given in Table II. The results reveal that there is a marginal improvement in Izod impact strength and energy with the incorporation of 5 phr PEEKMOH oligomer into the epoxy matrix. The increase may be due to the plasticization effect of PEEKMOH oligomer. However, with the incorporation of clay, the Izod impact energy and strength are decreased considerably. This is probably because of the incorporation of clay platelets into the epoxy matrix, the rigid nature will enhance and the plasticity will decrease on the resultant nanocomposites. Hence it is observed that though the nanoclay particles are effective in improving the modulus, they are not good enough to improve the Izod impact energy and strength of the resultant nanocomposites. Miyagawa et al.[46,47] have made similar observations for anhydride and amine-cured epoxy nanocomposites.

Thermogravimetric analysis

The thermal stability of the PEEKMOH-toughened epoxy clay ternary nanocomposites was studied by thermogravimetric analysis and the thermograms are given in Figure 5. From the figure, it reveals that the degradation started at 340°C for epoxy DDS system while, it was at 324°C for PEEKMOH-toughened epoxy DDS system, which may be due to decrease in crosslink density, but with incorporation of clay, the thermal stability of PEEKMOH-toughened epoxy DDS system increases as evidenced from the increase in onset of thermal degradation temperature with increase in clay content. This enhanced thermal stability may be ascribed due to the action of silicate layers as an effective barrier to the volatile products generated during decomposition and char formation

TABLE II
Izod Impact Energy and Strength of Epoxy Clay Ternary Nanocomposites

Composition	Impact energy (J)	Impact strength (J m^{-1})
Neat epoxy	0.146 ± 0.013	37 ± 3
Epoxy/PEEKMOH	0.154 ± 0.006	38 ± 2
Epoxy/Cloisite 25A (3 phr)	0.068 ± 0.010	19 ± 2
Epoxy/Cloisite 25A (1phr)/PEEKMOH	0.080 ± 0.020	20 ± 5
Epoxy/Cloisite 25A (3phr)/PEEKMOH	0.076 ± 0.011	19 ± 3
Epoxy/Cloisite 25A (5phr)/PEEKMOH	0.068 ± 0.003	17 ± 1

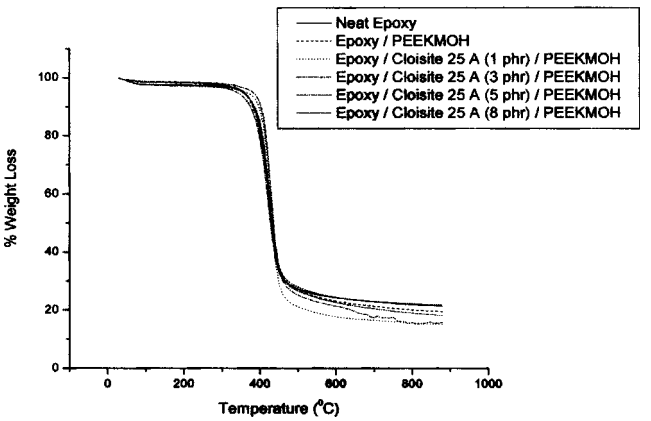

Figure 5 TGA thermograms of epoxy clay ternary nanocomposites.

Thermomechanical analysis

TMA was used to determine the coefficient of thermal expansion and T_g of the nanocomposites. Coefficient of thermal expansion (CTE) values of the nanocomposites is represented in Figure 6. It was observed that CTE values are decreasing with increase in clay content up to 3 phr, thereafter it increases. The decrease in CTE may be due to the uniform and nanolevel distribution of clay particles in epoxy matrix and also due to efficient stress transfer to clay layers. Surprisingly beyond 3 phr clay loading, the decrease in CTE was not observed considerably. This may be due to agglomeration of clay particles. No appreciable change in T_g was observed with the incorporation of clay into the epoxy matrix. However, DMA study reveals a considerable decrease in T_g with the incorporation of clay (Table III), which may be due to the plasticizing effect of organic moiety of clay particles thereby decreasing the crosslink density of epoxy network.

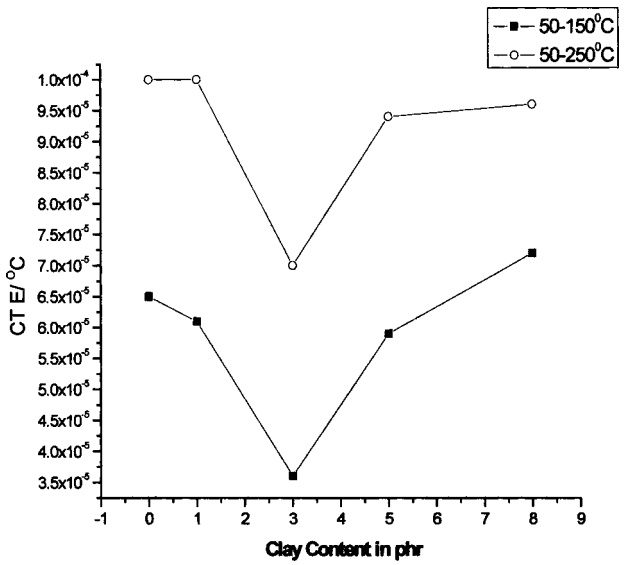

Figure 6 CTE versus clay content of epoxy ternary nanocomposite.

Dynamic mechanical thermal analysis

The viscoelastic properties of PEEKMOH toughened nanocomposites were investigated using a dynamic mechanical thermal analyzer. The tan δ curves for the PEEKMOH toughened nanocomposites are shown in Figure 7. The dynamic mechanical spectrum of the nanocomposites showed only a single T_g. Though two T_gs, corresponding to epoxy rich and thermoplastic-rich phases were expected as it was observed in our earlier paper on PEEKMOH toughened epoxy system,[23] only one T_g was observed because of the less percentage of PEEKMOH used and also due to the suppression of the mobility of thermoplastic fragments by rigid nanoclay layers. The T_g of the epoxy-rich phase decreased with the addition of PEEKMOH. This is due to the presence of a small amount of PEEKMOH remaining in the epoxy matrix. The decrease may be due to the decrease in crosslink density of the blends as a result of the reaction between epoxy and hydroxyl group of PEEKMOH.[23] It is further noticed that T_g is decreasing with increase in clay content in nanocomposites, which may be due to the plasticizing effect of organic modifier of clay layers. The storage modulus (E') and loss modulus (E'') were found to be higher for the nanocomposites below and above glass transition temperature compared to neat resin system (Figs. 8 and 9). The increase in the storage modulus and loss modulus were found to be about 92 and 33%, respectively for the composite system with 5 phr PEEKMOH and 5 phr nanoclay, when the temperature was less than glass transition temperature. This is due to the fact that exfoliation of nanoclay increases the interfacial interaction between the organic moiety of silicate layers and the epoxy matrix and PEEKMOH. However, beyond 5 phr of the nanoclay (8 phr of nanoclay), the improvement in storage modulus and loss modulus was reduced to 45 and 20%, respectively, due to the isolated clay aggrega-

TABLE III
T_g of the Ternary Nanocomposites

Composition	T_g (°C) DMTA (from tan δ)	T_g (°C) TMA
Neat epoxy	223	180
Epoxy/PEEKMOH	218	183
Epoxy/Cloisite 25A (3 phr)	221	183
Epoxy/Cloisite 25A (1phr)/PEEKMOH	216	180
Epoxy/Cloisite 25A (3 phr)/PEEKMOH	212	176
Epoxy/Cloisite 25A (5 phr)/PEEKMOH	217	177
Epoxy/Cloisite 25A (8 phr)/PEEKMOH	216	179

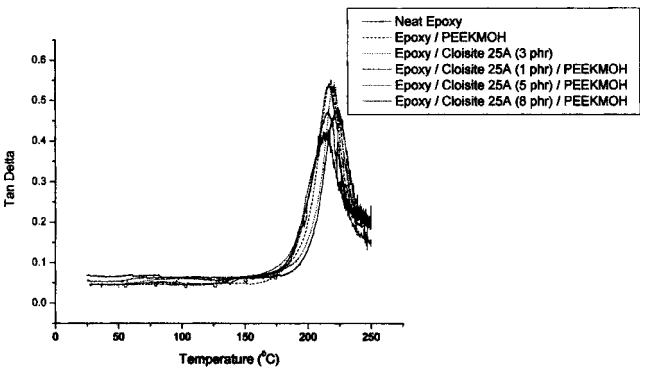

Figure 7 Tan δ versus temperature of epoxy ternary nanocomposites.

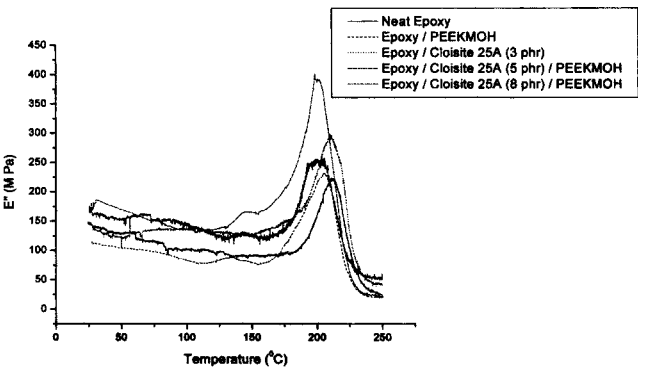

Figure 9 Loss modulus versus temperature of epoxy ternary nanocomposites.

tion, thereby declining the surface area of contact between polymer matrix and clay layers, in other words, interfacial interaction. The storage modulus was found to be lower for nanocomposite at T_g compared to that of neat epoxy system. This was a clear indication of lowering the crosslink density of the nanocomposite by the incorporation of PEEKMOH and nanoclay. Similar observation was made by us earlier for PEEKMOH[23] and PEEKTOH[24] toughened epoxy systems. Interestingly, loss modulus against temperature plot for nanocomposites revealed two peaks (Fig. 9). The peak between 130 and 160°C corresponds to the T_g of PEEKMOH rich phase and the peak at higher temperature corresponds to epoxy rich phase. The lowering of T_g was also observed in the loss modulus curve of nanocomposites with increase in clay content.

Scanning electron microscopy

Scanning electron microscopy was used for studying the morphology of nanocomposites. The scanning electron micrographs of cryogenically fractured surfaces of epoxy/5 phr PEEKMOH and epoxy/3 phr Cloisite 25A/5 phr PEEKMOH are shown in Figure 10(a,b), respectively. The cryogenically fracture surfaces were etched with chloroform to get a clear picture of the morphology. All the blends were heterogeneous. A two-phase morphology was clearly evident from the micrographs. No phase inversion or cocontinuous morphology was observed. The phase separation mechanism in epoxy resin/thermoplastic blends was studied extensively.[41,42] The phase separation mechanism was found to be dependant on the composition of blends, nature of curing agent, curing temperature, and a secondary phase separation was also observed in some cases. When the composition of blend was near the critical composition, phase separation occurred by spinodal decomposition and at off critical composition phase separation occurred by nucleation and growth mechanism. For thermoplastic with average molecular mass between 10,000 and 30,000 g/mol, the critical concentration of thermoplastic was 10–15% in liquid epoxy and diamine curator as calculated by Flory –Huggins model.[43] In the present study, PEEKMOH (Theoretical M_n = 12,000) was used at 5 phr to toughen the epoxy resin along with the Cloisite 25A, so the critical concentration may have been higher than the above mentioned range. Hence, the phase separation occurred by a nucleation and growth mechanism. Similar observations were made by us earlier for PEEKTOH[24]- and PEEKMOH[23]-toughened epoxy systems. Here, gelation followed by vitrification occurred after the phase separation. It was found that the domain size of PEEKMOH decreased with the addition of nanoclay. The viscosity of the system will increase with the addition of clay and the mobility will decrease with the progress of curing reaction. In highly viscous system, gelation could occur at an early stage giving rise to smaller domains. After the initial formation of the domains, coalescence of the separated domains takes place if the viscosity is low enough and results in large domains. In highly viscous systems, the extent of

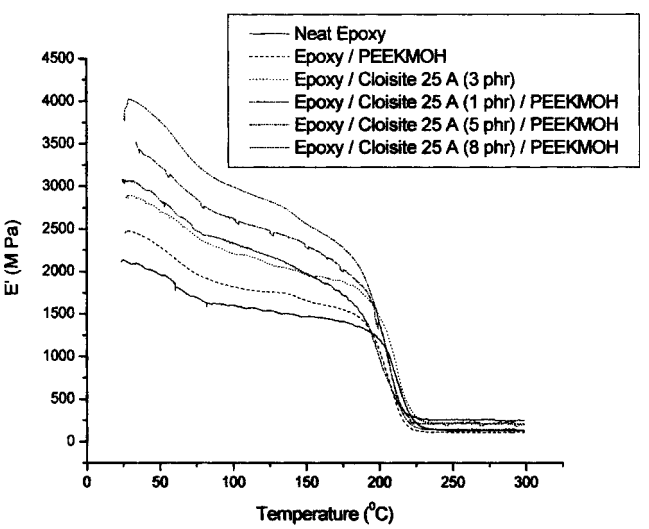

Figure 8 Storage modulus versus temperature of epoxy ternary nanocomposites.

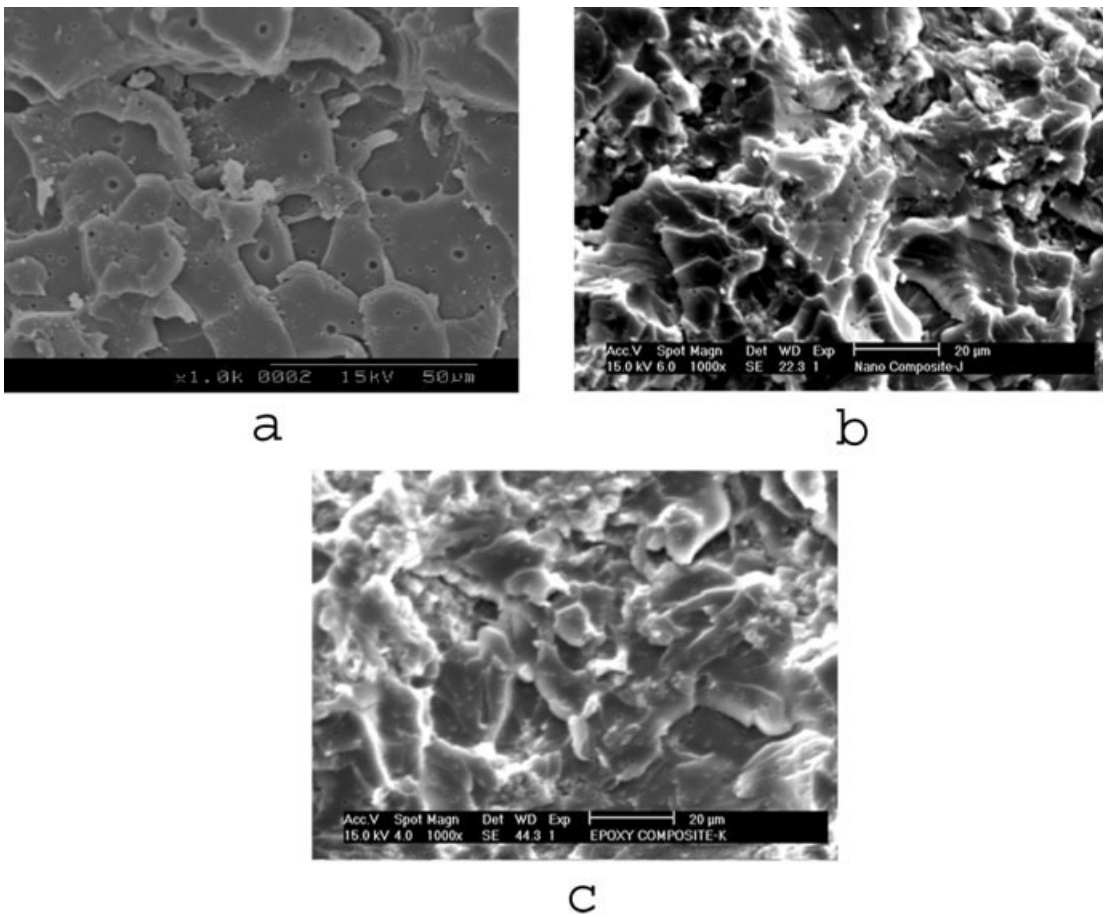

Figure 10 SEM images of cryogenically fractured surfaces of (a) epoxy/5 phr PEEKMOH, (b) epoxy/3 phr Cloisite 25A/5 phr PEEKMOH, and (c) epoxy/5 phr Cloisite 25A/5 phr PEEKMOH.

coalescence was less, and as a result, the domain size will be small. As the clay content increases, the phase separation was disappeared. This may be due to the faster cure reaction of epoxy amine in the presence of nanoclay, which is acidic, resulting in highly viscous systems at a faster cure rate. In other words, gelation occurs before phase separation (the rate of gelation is faster than the phase separation).

The SEM micrograph of the tensile failed specimens of neat epoxy, epoxy/PEEKMOH, epoxy/3 phr Cloisite 25A, and epoxy/5 phr Cloisite 25A/5 phr PEEKMOH are shown in Figure 11(a–d), respectively. The fracture surface of neat epoxy resin showed typical characteristic of brittle fracture. The surface was smooth and crack propagation uninterrupted. The failure surface of epoxy/5 phr PEEKMOH, epoxy/3 phr Cloisite 25A, and epoxy/5phr Cloisite 25A/5 phr PEEKMOH were rough and ridge patterns and river markings could also be seen on the fracture surface. The roughness of the fracture surface was due to two reasons. First, it is an indication of crack path deflection i.e., the crack deviated from its original plane, increasing the area of crack. Hence, the energy required for propagation of the crack increased. Second the roughness indicated the ductile nature of the crack. The matrix became less brittle in comparison with the unmodified epoxy because of a decrease in the crosslink density. The polar hydroxyl groups of PEEKMOH enhanced the interfacial adhesion either through the opening of epoxy ring or through the hydrogen-bonding interactions between the matrix and oligomer as it was observed in our earlier publication.[23] Another factor responsible for the increase in the fracture toughness was the local plastic deformation of the matrix. The dispersed domains acted as stress concentrators, and this led to the plastic deformation of the matrix surrounding the domains. According to Hedrick et al.,[44] river markings on the fracture surface were an indication of plastic deformation of the matrix. On careful observation of Figure 11(d), it reveals that clay incorporation into the PEEKMOH toughened epoxy system, the pulling out of thermoplastic phase on etching with chloroform has been reduced and pulling out totally disappeared with 5 phr clay incorporation. At the same time, the river markings are increased with clay incorporation into the PEEKMOH toughened epoxy system. This may be due to the uniform dispersion of clay in nano

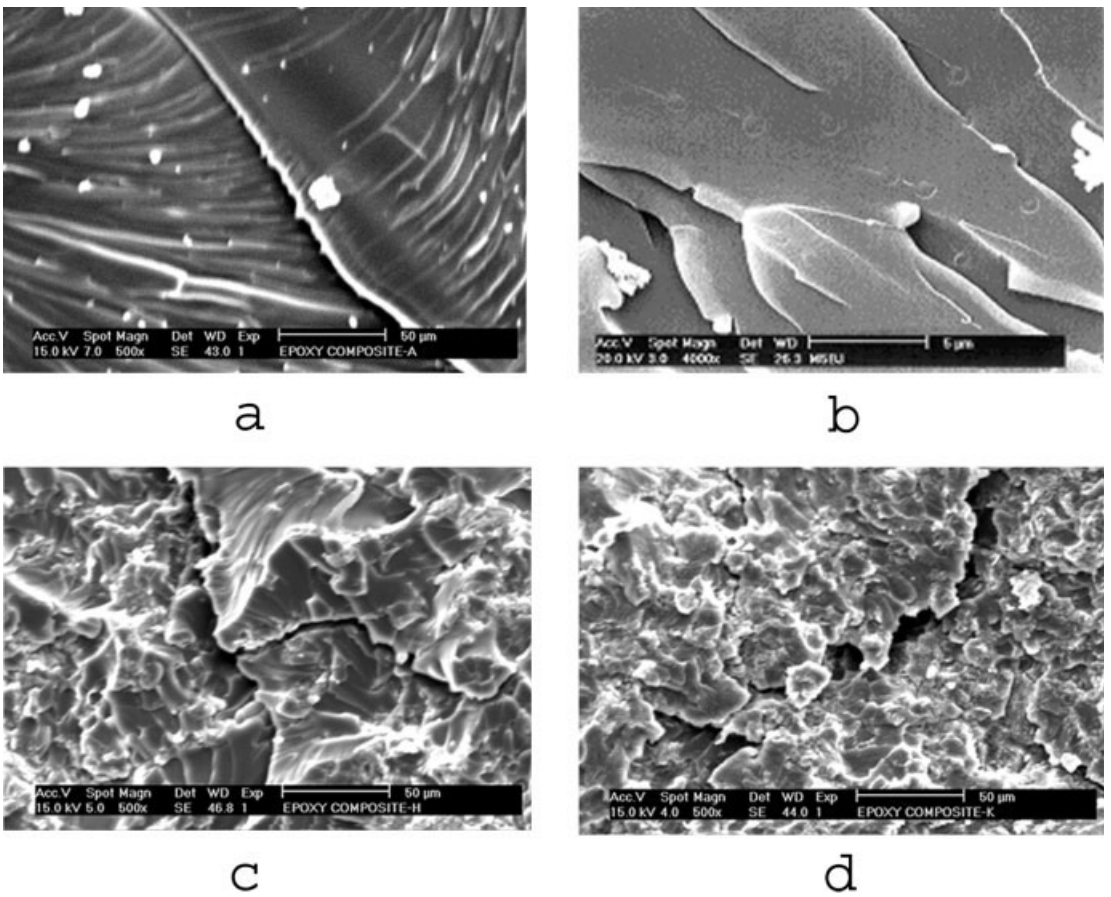

Figure 11 SEM images of tensile-failed surfaces of (a) neat epoxy, (b) epoxy/5 phr PEEKMOH, (c) epoxy/3 phr Cloisite 25A, and (d) epoxy/5 phr Cloisite 25A/5 phr PEEKMOH.

and exfoliated manner all through the matrix and prevents the pulling out of thermoplastic phase at the same time restricting the crack propagation more efficiently. Hence, both thermoplastic and clay are influencing the fracture behavior and toughness of ternary nanocomposites.

CONCLUSION

- PEEKMOH toughened epoxy clay ternary nanocomposites were processed by melt-mixing of PEEKMOH with epoxy along with clay with mechanical stirring followed by ultrasonication.
- X-ray diffraction studies reveal a complete exfoliated structure for all nanocomposites even for higher loading of clay.
- Tensile and flexural moduli were increased with increase in clay content. However, there is a marginal decrease in tensile strength as the clay content increases. Percentage strain at break and fracture toughness were found to be higher for PEEKMOH toughened epoxy clay ternary nanocomposites compared to neat epoxy resin.
- Izod impact energy and strength were decreased considerably with the incorporation of clay.
- Storage modulus and loss modulus were found to be higher for the nanocomposites below and above glass transition temperature compared to neat resin system indicating better interaction between the phases.
- The lowering of T_g was observed with increase in clay content in the dynamic mechanical spectrum of blends.
- The CTE values are decreasing with increase in clay content up to 3 phr thereafter it increases.
- Scanning electron microscopy reveals that phase separation occurred by nucleation and growth mechanism. As the clay content increases to 8 phr, phase separation disappears confirming that gelation occurs before phase separation.
- Various toughening mechanisms like crack path deflection, ductile nature of crack, and plastic deformation of the matrix are playing a major role for the increase in toughness of nanocomposites.
- Marginal improvement in thermal stability was observed with increase in clay content.

The authors thank Dr. B. N. Suresh, Director, Vikram Sarabhai Space Centre (VSSC) for giving permission to publish the article. One of the authors (A. Asif) is thankful to Dr. G. Madhavan Nair, Chairman, Indian Space Research Organisation and Dr. B. N. Suresh, Director, VSSC for providing ISRO Research fellowship. Thanks to all colleagues of Analytical and Spectroscopy Division and Material Characterisation Division of VSSC, Regional Research Laboratory, Thiruvananthapuram and Sree Chitra Tirunal Institute for Medical Sciences and Technology, Biomedical Technology Wing, Thiruvananthapuram for analytical support.

References

1. Ray, S. S.; Okamoto, M. Prog Polym Sci 2003, 28, 1539.
2. Zeng, Q. H.; Yu, A. B.; Lu, G. Q.; Paul, D. R. J Nanosci Nanotechnol 2005, 5, 1574.
3. LeBaron, P. C.; Wang, Z.; Pinnavaia, J. T. Appl Clay Sci 1999, 15, 11.
4. Alexandre, M.; Dubois, P. Mater Sci Eng 2000, 28, 1.
5. Hackman, I.; Hollaway, L. Compos A, to appear.
6. Vaia, R. A.; Giannelis, E. P. MRS Bulletin, May 2001, pp 294–301.
7. Gao, F. Mater Today 2004, 7, 50.
8. Ogasawara, T.; Ishida, Y.; Ishikawa, T.; Aoki, T.; Ogura, T. Compos A, to appear.
9. Campbell, S. G.; Johnston, C. NASA Glenn's Research and Technology Reports, Updated 2004.
10. Jiankun, L.; Yuacai, K.; Zongneng, Q.; Xiao-Su, Y. J Polym Sci Part B: Polym Phys 2001, 39, 115.
11. Xu, W.-B.; Bao, S.-P.; He, P.-S. J Appl Polym Sci 2002, 84, 842.
12. Kornmann, X.; Lindberg, H.; Berglun, L. A. Polymer 2001, 42, 4493.
13. Lan, T.; Kaviratna, P. D.; Pinnavaia, T. J. Chem Mater 1995, 7, 2144.
14. Ryu, J. G.; Park, S. W.; Kim, H.; Lee, J. W. Mater Sci Eng C 2004, 24, 285.
15. Lam, C.-K.; Lau, K. T.; Cheung, H. Y. Ling, H. Y. Mater Lett 2005, 59, 1369.
16. Zunjarrao, S. C.; Sriraman, R.; Singh, R. P. J Mater Sci 2006, 41, 2219.
17. Yasmin, A.; Abot, J. L.; Daniel, I. M. Scripta Mater 2003, 49, 81.
18. Velumurugan, R.; Mohan, T. P. J Mater Sci 2004, 39, 7333.
19. Lu, H. J.; Liang, G. Z.; Ma, X.-Y.; Zhang, B.-Y.; Chen, X.-B. Polym Int 2004, 53, 1545.
20. Park, J. H.; Jana, S. C. Macromolecules 2003, 36, 2758.
21. Francis, B.; Vandenpoel, G.; Posada, F.; Groeninckx, G.; Rao, V. L.; Ramaswamy, R.; Thomas, S. Polymer 2003, 44, 3687.
22. Francis, B.; Rao, V. L.; Vandenpoel, G.; Posada, F.; Groeninckx, G.; Ramaswamy, R.; Thomas, S. Polymer 2006, 47, 5411.
23. Francis, B.; Thomas, S.; Jose, J.; Ramaswamy, R.; Rao, V. L. Polymer 2005, 46, 12372.
24. Francis, B.; Thomas, S.; Asari, G. V.; Ramaswamy, R.; Jose, S.; Rao, V. L. J Polym Sci Part B: Polym Phys 2006, 44, 541.
25. Zhang, K.; Wang, L.; Wang, F.; Wang, G.; Li, Z. J Appl Polym Sci 2004, 91, 2649.
26. Mimura, K.; Ito, H.; Fujioka, H. Polymer 2000, 41, 4451.
27. Pasquale, G. D.; Motta, O.; Rocca, A.; Carter, J. T.; McGrail, P. T.; Acierno, D. Polymer 1997, 38, 4345.
28. Barral, L.; Cano, J.; Lopez, J.; Bueno, I. L.; Nogueira, P.; Ramirez, C.; Torres, A.; Abad, M. J. Thermochim Acta 2000, 344, 147.
29. Bennet, G. S.; Faris, R. J.; Thompson, S. A. Polymer 1991, 32, 1633.
30. Wu, S. J.; Tung, N. P.; Lin, T. K.; Shyu, S. S. Polym Int 2000, 49, 1452.
31. Wu, S. J.; Lin, T. K.; Shyu, S. S. J Appl Polym Sci 2000, 75, 26.
32. Blanco, I.; Cicala, G.; Faro, C. L.; Recca, A. J Appl Polym Sci 2003, 89, 268.
33. Frohlich, J.; Thomann, R.; Mulhaupt, R. Macromolecules 2003, 36, 7205.
34. Balakrishnan, S.; Start, P. R.; Raghavan, D.; Hudson, S. D. Polymer 2005, 46, 11255.
35. Isik, I.; Yilmazer, U.; Bayram, G. Polymer 2003, 44, 6371.
36. Peng, M.; Li, H.; Wu, L.; Chen, Y.; Zheng, Q.; Gu, W. Polymer 2005, 46, 7612.
37. Allcock, H. R.; Lampe, F. W.; Mark, J. E. Contemporary Polymer Chemistry; Englewood Cliffs, NJ: Pearson Prentice Hall, 2003.
38. Jurek, M. J.; McGrath, J. E. Polymer 1989, 30, 1552.
39. Park, J. H.; Jana, S. C. Macromolecules 2003, 36, 8391.
40. Basara, C.; Yilmazer, U.; Bayram, G. J Appl Polym Sci 2005, 98, 1081.
41. Blanco, I.; Cicala, G.; Faro, C. L.; Recca, A. J Appl Polym Sci 2004, 94, 361.
42. Overbeke, E.; Devaux, J.; Lrgras, R.; Carter, J. T.; Mc Grail, P. T.; Carlier, V. Polymer 2003, 44, 4899.
43. Bonnet, A.; Camberlin, Y.; Pascault, J. P.; Sautereau, H. Macromol Symp 2000, 149, 145.
44. Hedrick, J. L.; Jurek, M. J.; Yilgor, I.; McGrath, J. E. Polym Prepr 1985, 29, 293.
45. Wang, K.; Chen, L.; Wu, J.; Toh, M. L.; He, C.; Yee, A. F. Macromolecules 2005, 38, 788.
46. Miyagawa, H; Drzal, L. T. J Adhes Sci Technol 2004, 18, 1571.
47. Miyagawa, H; Foo, K. H; Daniel, I. M; Drzal, L. T. J Appl Polym Sci 2005, 96, 281.